Egyptian Journal of Archaeological and Restoration Studies (*EJARS*)
An international peer-reviewed journal published bi-annually
www.ejars.sohag-univ.edu.eg

Original article

USING THE GREEN NANOCOMPOSITE IN THE RESTORATION OF OIL PAINTINGS: APPLIED TO A 20TH CENTURY HISTORICAL OIL PAINTING.

Abo Taleb, Th.[1(*)] & Sabry, W.[2]

[1]*Conservation dept., Faculty of Archaeology, Aswan Univ., Aswan*
[2]*Polymers & Pigments dept., National Research Centre, Dokki, Giza, Egypt*
**E-mail address: drthanaaabotaleb@arc.aswu.edu.eg*

Article info.

Article history:
Received: 19-7-2024
Accepted: 1-10-2024
Doi: 10.21608/ejars.2025.471784

Keywords:
Silica nanoparticles
Degradation
Consolidation
Cellulose nanofibers
SNP

EJARS – Vol. 15 (2) – Dec. 2025: 197-208

Abstract:

The layers of oil paintings are exposed to inappropriate environmental changes that result in the degradation of paintings and the acidity of the canvas, causing the loss of mechanical properties of canvas oil paintings and the deterioration of the layer painting. Oil paintings can be restored using green nanocomposite and treated using nanocomposite loaded on a polymer added with other compatible nanomaterials. This leads to the penetration of the treated material and the homogeneous surface. The green nanocomposite consists of polyelectrolyte-treated silica nanoparticles (SNP) and cellulose nanofibers (CNF) to strengthen the fabric and colors. Nanocomposite is a form of a film of CNF on the surface of the paint, which increases ductility, but without deep penetration. Thus, an additional component was introduced, i.e., SNP, for its ability to penetrate fiber. The present research paper discusses changing the SNP/CNF ratio to achieve appropriate reinforcement on experimental samples with different ratios (1:1, 9:1, and 1:9) to test the CMS@SNP/ CNF nanocomposite, and the materials were evaluated by measuring the mechanical properties. Moreover, tests and analyses of the layers of the painting, such as microscopic examination, SEM-EDX, Raman analysis, and assessment of the damage to the painting, were carried out to treat and restore the historical painting scientifically. The FTIR, colorimeter, and microscopic examination of the samples before and after photothermal aging and thermal aging confirmed the suitability of using the nanocomposite in a ratio of 1:9 and applied to a painting of the twentieth century (20 cm×50 cm) with cuts, gaps, weak texture, and falling off color crust.

1. Introduction

Paintings on canvas have been exposed to damage over time due to changes in improper environmental conditions [1], which have led to cracking of the paint layer, tearing and weakening of the canvas, damage to the painting, and loss of the mechanical properties of the canvas support. The restoration process was carried out by consolidation or lining [2]. In both cases, the treatment was conducted with an adhesive, probably natural, such as animal glue, or a synthetic adhesive, such as acrylic (Plexisol PB550, Paraloid B72, and Plextol B500) [3]. Complex compositions of wax and resin (371 Beva or water-based adhesives) are less preferred due to the hygroscopic nature of the cellulose canvas, which causes swelling and shrinkage of the canvas as a reaction to interactions with water, leading to changes in the dimensions of the painting and some synthetic adhesives, such as polyvinyl acetate and deterioration of the canvas due to acidic products formed during decomposition [4]. Therefore, they are no longer used. Despite the sensitivity of the canvas to water towards waterborne [5,6] treatments, nanomaterials dissolve in water, which are very effective even at low concentrations. Because of their small size, they penetrate the material to be treated well [7]. The use of nanomaterials in consolidation, cleaning [8], and deacidification [9] has increased, using calcium and magnesium hydroxide/carbonate nanoparticles [10] to remove acidity well [11]. Nano-titanium dioxide and nano-zinc oxide protect against fungal growth and ultraviolet radiation. Additionally, treatment with colloidal nano-silica solutions plays a role in the stability and consolidation of wood [12]. Good colloidal stability (colloidal is a type of mixture in which small particles of a substance are suspended and dispersed through a continuous medium) is essential. It constitutes a prerequisite for surface consolidation of oil paintings using colloidal nano-silica based on the use of nanoparticles for mechanical reinforcement of fibers as a material loaded on a polymer added with other compatible nanomaterials, which leads to the penetration of the treated material and a homogeneous surface [13]. The incompatibility of the nanomaterials with the surface decreases the treatment efficiency. Improving stability and chemical compatibility by changes in pH ionic strength or adsorption on a degraded surface [14] and fusion is often achieved by the adsorption of oppositely charged polyelectrolytes [15]. How-

ever, this may lead to flocculation between the fibers due to the strong electrostatic interactions between the molecules and the polymer chains [16]. After adsorption, the particles are equalized and lack electrostatic repulsion leading to order and conformation on the surface [17]. The use of nanocellulose in reinforcement is often due to its unique mechanical properties and surface features, such as gas, grease barrier, or hydrophobic, antibacterial, and anti-ultraviolet behaviors. Cellulose nanofibers (CNFs) have high strength [18] and form transparent and lightweight membranes. In addition, they have large surface areas, which can be modified in sophisticated ways [19]. Strengthening the canvas cellulose with a material of a similar nature is useful for the preservation of canvas and has many advantages compared to ordinary cellulose fibers since CNFs are much lighter and have more extensive mesh structures [20], which leads to higher mechanical properties of the film and a tensile strength of up to 310 MPA [21]. Nano-cellulose has been incorporated as a reinforcing agent in various polymer matrices recently to unify historic papers [22]. To fulfill consolidation purposes, it has been used as a 2.5% CNF reinforcing material for the colored and back surface of the painting after proving its success by evaluating its efficiency after conducting tests from colorimetry, luminometry, ART-FTIR, and Raman spectroscopy to determine the effects of heat and humidity on the paint layer. It has been proven that CNFs have a good unifying effect with no discoloration [23]. Its disadvantages reveal that they do not penetrate to the depths, so materials, such as silica nanoparticles, are added to improve their performance [24] and penetrate more [25] because these materials are abundant, non-toxic, and inexpensive [26]. It has been proven to be a good strengthening agent for other fibrous materials, such as paper and canvas [27], that have an alkaline nature [28] and may provide deacidifycation. Both components have been shown to provide good reinforcement on paper [29] and cotton canvas when used individually [30]. CNFs are similar to the same chemical nature canvas. Therefore, they interact well with the surface of fibers [31] and nano-cellulose fibers of aqueous formulations that provide mechanical stability [32] by enabling a network of hydrogen bonds formed on the surface of the canvas, causing mechanical improvement [33].The network of cellulose nanoparticles and their interaction with textiles and the anionic polymer (carboxymethyl) cellulose (CMC) is added, and the cationic polymer (PEI) polyelectrolyte, as the previous hydrogen bond to strengthen using a procedure that allows the formation ending with a layer of a cellulosic nature. The CMC outer layer makes the SNP negatively charged, preventing flocculation with negatively charged CNF and proving to be better under normal conditions [34]. PEI tends to turn yellow at temperatures above 100oC or when exposed to ultraviolet radiation. Its concentration is reduced to a minimum under normal conditions in the CMC@SNP [35] preparation so that no discoloration can be observed. CNFs are more effective than cellulose nanocrystals (CNCs) as coating layers with a higher aspect ratio, allowing CNFs to organize more tightly an interlocking network. On the contrary, CNCs have a fragile stacked structure (film) due to the inability to form interlocking networks [36]. So, aqueous compositions are applied to the surface of the painting from CMC@SNP: CNF in different ratios of 9:1, 1:1, and 1: 9. When CNF is added, the silica concentration decreases. CNF remains on the surface of the fabric, while silica penetrates the fabric. As the silica content decreases, the viscosity decreases, allowing deeper transmission, and the composition achieves a mass ratio of CMC@SNP CNF: 1:9. The fracture strength increases, the elongation at fracture decreases slightly, and the best mechanical performance is obtained. The combined nanocomposites of SNP and CNF treated with CMC have proved to be suitable for effectively addressing the loss of mechanical integrity of the deteriorating canvas [37].

2. Materials & Methods

2.1. *Materials*

An analytical examination study was carried out for 3 samples of yellow, red, and green falling from a historical painting in the twentieth century as the case study. Experimental samples were also made, and nanomaterials equipped in the laboratory of Nano-polymeric materials - National research center - Egypt, which were applied to them. Additionally, industrial aging was carried out on them, and the efficiency of nanomaterials in strengthening and deacidification was evaluated. Then, the application was carried out on the historical painting.

2.2. *Methods (Application of the consolidates to the simulated samples).*

The following specifications materials were used Cellulose Nanofiber with molecular formula $(C_6H1_0O_5)_n$, average size 10:20 nm and density 1.5 g/cm3 was supplied from Aritech Chemazone Pvt Ltd, 890, Sector 7, Urban Estate, Kurukshetra, India , Silica nanoparticle with molecular formula SiO_2, average size 15:20 nm, molecular weight 60.08 g/mol , polyethyleneimine (PEI) having a weight average molecular weight of 25000 g/mol were purchased from Sigma-Aldrich Chemie GmbH. Eschenstr. 5, 82024 Taufkirchen, Germany, Carboxy methyl cellulose with methyl content less than 10% and 10% moisture in addition to viscosity 5000 MPA.S was supplied from Hebei Tangpeng Co., Ltd. Zhongshan East Road, Shijiazhuang Hebei, China, Marathon ion exchange resin was supplied from Scientific Laboratory Supplies Ltd. Greenogue Business Park, Rathcoole, Dublin, Ireland, Sodium hydroxide was molecular formula NaOH was purchased from El-Nasr chemical company – Cairo – Egypt.

2.2.1. Preparing the nanocomposite

The nanocomposite was processed, fig. (1), as follows: **1st step**, preparation of electrolytic silica particles: Electrolytic silica particles are characterized by the ability to disperse in solution and are prepared using 1% silica solution with ethyl alcohol at a concentration of 40% to make ion exchange with marathon resin to reach pH 3 to ensure that there are no charges on the surface of silica particles. Twenty-five microliters of polyethylene amine solution with a concentration of 4.7% were added to give the ability to silica molecules to adsorb 1.86 ml of polycarboxymethyl cellulose in the presence of sodium hydroxide solution with a concentration of 0.1 caliber to raise the pH value of the number 11. Thus, the

treated electrolytic silica particles were obtained at a concentration of 4.5 %. **2nd step**, the silica electrolytic particles were mixed with cellulose nanometer fibers [Sil /PEI/CMC: CNF/w: w] in different proportions 1:9, 1:1, 9:1. It is used in consolidation with a concentration of 2.5%. **3rd step,** the processing of experimental samples and aging procedure: The Belgian linen canvas was used, and the number of warp and weft threads was 13×15 cm^2. The samples measured 0.7 (thickness) × 7 (width) × 15 (length), 54 samples were prepared to measure the mechanical properties of the samples treated after thermal and light aging and compare them with the standard samples. They were divided as follows: ***)** For Elongation measurement test, 27 samples. 9 samples were tested after thermal aging, 3 samples for each treatment (nano material) and the average were taken. Also, 9 samples were tested after optical aging and the average was taken. 9 standard samples were tested and the average was taken. ***)** For the breaking force test, 27 samples were prepared as follows:9 samples, 3 for each treatment after thermal aging and the average was calculated. 9 samples, 3 for each treatment after optical aging and the average was calculated. 9 standard samples, 3 for each treatment for the fracture test and the average was calculated.

Figure (1) the stages of preparing nanomaterials in the laboratory

The degradation of the fabric samples was carried out by bleaching the fabric to mimic the natural processes of oxidation and hydrolysis of cellulose catalyzed by acid [38] by immersing the pieces of fabric in a glass basin with a mixture of 200 ml of hydrogen peroxide at 35 wt% and 10 ml of sulfuric acid (95-97 wt%) for 72 hours at 40 °C with light stirring. Upon completion, the fabric was thoroughly rinsed with water to remove grease residues (such as grease or mineral oil). Then, the fabric was aged after applying the ground layer and the paint layer of the same colors. In a thermal aging furnace at 90 °C and 65% relative humidity (RH) for 18 days, fig. (2-a:d). The compressive strength and the flexural resistance force were measured. Then, the nano-composite of the Sil /PEI/CMC: CNF was applied with a brush on the surface by 1:9 /9:1/1:1. Two layers of treatment were used to strengthen the color crust before the industrial aging process, which was carried out by exposing the samples to a **T** of 60°C and **RH** of 80 % for 240 hours. Other samples were exposed to ultraviolet radiation for 240 hours (10 days) [39], which equaled 50 years using a mercury bulb (E40-F500 W), and the type of ultraviolet radiation used UVA: 5.5616 mw/cm^2 = 268-365 nm.

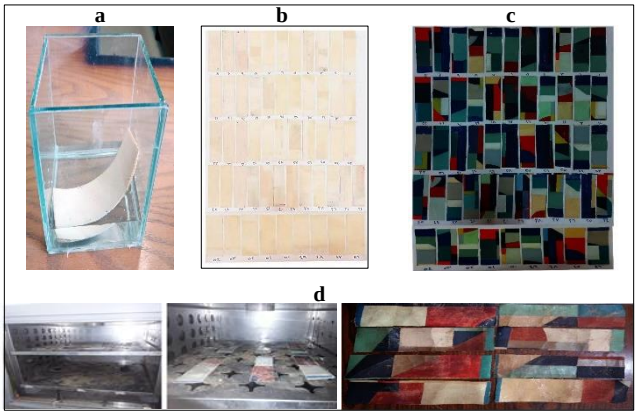

Figure (2) the stages of preparing the sample **a.** & **b.** the bleaching stage the textile before and after bleaching, **c.** the samples after paint layers' application, **d.** some samples after aging

2.2.2. Microscopic examination

The examination of the historical painting was carried out with a polarized microscope (model: Nikon polarizing microscope eclipse lv100pol) and a light microscope. The expe-rimental samples were evaluated through the morphological surface by SEM (Model JEOL JSM 5400 LV EDX Link ISIS - Oxford detector "high vacuum") to assess the success of reinforcing materials and observation of the suitability of reinforced materials before and after application and examination of archaeological samples in historical painting.

2.2.3. Measurement of the pH value

The pH value was measured using a digital portable pH meter, and the evaluation was carried out before treatment on the obsolete sample and the treated sample before and after aging.

2.2.4. Color measurement

The color change measurement was carried out to evaluate the reinforced materials before and after industrial aging, note the suitability of the reinforced, and remove acidity materials. The evaluation was carried out before treatment on the obsolete sample and the treated sample before and after aging. Color measurements were made before and after treatments using CM 2600d spectrophotometer (Konica Minolta). The L*a* and b* analog spectropho-tometer measured the samples according to the L*a*b* color space using three Xenon-flash lamps. The CIE L*a*b* color space describes the colors visible to the human eye in three coordinates. L* describes the lightness of the color from 0-black to 100-white, a* describes the location between red and green, and b* describes the location between yellow and blue.

2.2.5. Measurement of mechanical properties

The evaluation was carried out before treatment on the aging sample and the treated sample before and after aging. To assess the success of the reinforcing materials on the experimental sample, the tensile strength and elongation were measured with the AG-X autograph table - Top type - Shimadzu - Japan, at a relative humidity of 60% and 23 °C for 24 h. Three measurement points were scored for each percent of the elongation, and the average was taken. Considering the cutting direction, it is uniform in all samples, three measurements are made, and then the average measurement accuracy and

elongation are usually taken on the stand ranging from (0-300 Newton) / and (0-3%) [40]. These values corresponded to the limit after which the canvas brought to be torn.

2.2.6. Infrared and Raman analysis

FTIR (model Bruker'S VERTEX 70V FT-IR Spectrometer Resolution 4) was used for the infrared analysis of samples before and after aging on three regions in the analysis−a region of 2700-3600, expressing the hydroxyl group [41] the aliphatic hydrocarbon, the absorption zone (1470-1820) characteristic of the cellulose group, and the absorption zone of 800-1490 cm^{-1} [42]and expressing the spectra of typically. Cellulose molecules contain a high amount of OH bonds to the hydroxyl group, and CH bonds are specifically present in about 3300 cm^{-1} and 2900 cm^{-1} to the hydrocarbon group. Archaeological samples of historical paintings and varnishes were analyzed using a laser with a wavelength of 780 nm to identify the chemical composition of the material molecule for both inorganic and organic materials. After examination and analysis, the damage condition was evaluated and restored.

3. Results

3.1. *SEM examination results*

The microscopic examination of the treated samples before aging and after aging showed the diffusion of the nanocomposite CNF: Sil /PEI/CMC and the penetration of silica in the applied sample in a ratio of 9:1. There was shrinkage and non-penetration of the reinforcing material in the applied sample in a ratio of 1:1 and 1:9. Additionally, silica atoms appeared on the surface after application, fig. (3).

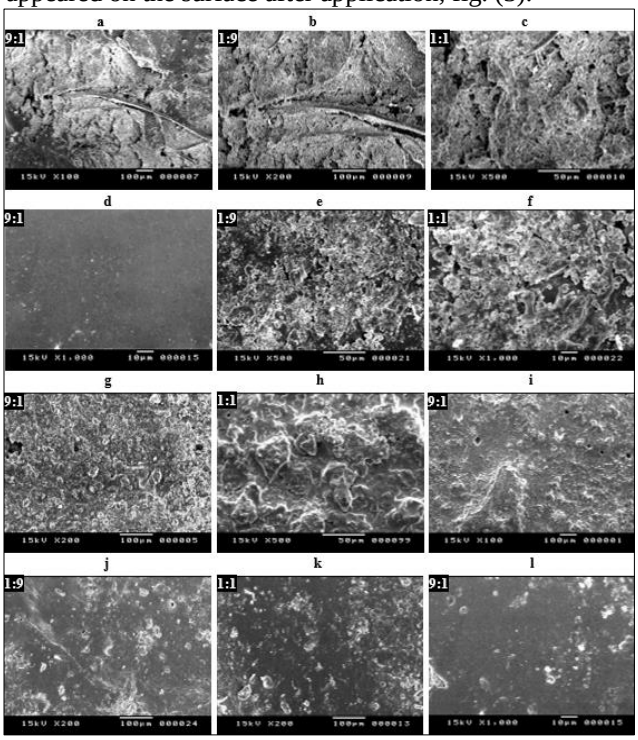

Figure (3) SEM photomicrographs; **a.**, **b.** & **c.** samples before thermal ageing with the application of the nanomaterial with different ratios, **d.**, **e.** & **f.** samples after thermal aging, **g.**, **h.** & **i.** sample, before lighting aging after application of the nano-material in different ratios, **j.**, **k.** & **l.** samples after lighting aging after application of the nanomaterial

3.2. *pH value results*

Surface pH was measured, and the pH was 5.5, so deacidification treatment was generally necessary on the fabric from the back surface. Pre-treatment evaluation was performed on the aging sample and the treated sample before and after aging, tab. (1). The measurement result revealed that an alkaline reserve was deposited on the surface of the sample, and the pH was alkaline when the mixing ratio was 1:9. The other samples were acidic in other mixing ratios of 1:1/1:9.

Table (1) result of pH values of untreated samples and treated samples before and after aging

Nanocomposite ratio	pH of none treated samples	pH of treated samples by nanomaterial before aging	pH of treated samples by nanomaterial after aging
--	--	--	5.5
	Effect of thermal aging		
9:1 [Sil /PEI/CMC: CNF]	5.5	8	9
1:9 [Sil /PEI/CMC: CNF]	5.5	6	6.2
1 [Sil /PEI/CMC: CNF]:1	5.5	5	6
	Effect of lighting aging		
9:1[Sil /PEI/CMC: CNF]	5.5	8	8.5
1:9 [Sil /PEI/CMC: CNF]	5.5	5.6	5.9
1:1[Sil /PEI/CMC: CNF]	5.5	5.7	5.5

3.3. *Color measurements results*

The color difference was evaluated before treatment on the aging sample and the treated sample before and after aging. It was found that the least change in color after aging was in a sample at a ratio of 9:1 compared to other samples at a ratio of 1:1/1:9, tab. (2).

Table (2) result of color measurements

Ratio before the treatment	L*	a *	b*	ΔE after treatment
	Untreated sample			
	90.7	-0.2	0.1	-
	Effect of thermal aging of the treated samples			
9:1 before aging	90.1	-0.2	0.1	**0.6**
9:1 after aging	91.5	-0.3	0.3	**0.8**
1:9 before aging	90.1	-0.4	1.4	**1.3**
1:9 after aging	90.2	-0.5	1.5	**1.5**
1:1 before aging	90.5	-0.21	1.1	**1.0**
1:1 after aging	90.7	-0.3	1.2	**1.1**
	Effect of lighting aging of the treated samples			
9:1 before aging	90.3	-0.3	0.3	**0.45**
9:1 after aging	90.4	-0.4	0.4	**0.9**
1:9 before aging	90.1	-0.5	1.6	**1.4**
1:9 after aging	90.1	-0.6	1.7	**3.2**
1:1 before aging	92.3	-0.4	1.2	**1.06**
1:1 after aging	92.5	-0.6	1.4	**5.11**

3.4. Mechanical properties results

Mechanical testing of experimental samples was carried out before treatment on the obsolete sample, and the sample was treated with the combined compound of nanomaterials before and after aging to assess the differences in the fracture strength of the material and elongation of experimental samples after thermal and light aging. The results are shown in tab. (3). The results indicated that the resistance [CMC@SNP: CNF (w/w)] with a 9:1 ratio of fracture strength and elongation was greater than other ratios 1:1/1:9 used after industrial obsolescence. As a result of exposure of sample at ratio 9:1 [CMC@SNP: CNF (w/w)] to heat and relative humidity, the fracture strength increased by 43.6% (from 4.24 to 6.09 KN/m), while the elongation was reduced (from 35.4 to 33.1%). Exposure to UV rays increased by 45.4% (from 4.24 to 6.15 KN/m), while the elongation was reduced (from 35.4 to 33.5%), which was one of the best results. For the sample at ratio 1:9, the fracture strength increased by 17.8% (from 4.24 to 4.95), and elongation increased (from 35.4 to 38.5). As for exposure to UV rays, the fracture increased by 19.8% (from 4.24 to 5.08 KN / m), while the elongation was increased (from 35.4 to 37.8%).

For the sample at ratio 1:1, the fracture strength was increased by 20.1% (from 4.24 to 5.09), and the elongation decreased (from 35.4 to 39.3). UV exposure increased by 20.2% (from 4.24 to 5.10 KN/m), while the elongation was reduced (from 35.4 to 37.6%).

Table (3) measurement of the breaking strength of linen canvas before and after treatment by nanocomposite

CMC@SNP: CNF (w/w)	Elongation at break (%)	Breaking force (kN/m)
Non treated samples	35.4	4.24
Effect of thermal aging on the treated samples		
1:9	**38.5**	**4.95**
9:1	33.1	6.09
1:1	39.3	50.9
Effect of lighting aging on the treated samples		
1:9	37.8	5.08
9:1	33.5	6.15
1:1	37.6	5.10

The analysis, tab. (4) & fig. (4) showed that the sample treated with a ratio of 9:1 [CMC@ SNP: CNF (w/w)] revealed no change in the chemical composition because both the hydroxyl group and C-H stretching slightly increased compared to others, suggesting that the water content of cellulose was not affected by the canvas. Moreover, the C=O group did not change, denoting no effect on the hemicellulose group. There was a change in the chemical composition in the samples at a ratio of 1: 1 [CMC@SNP: CNF (w/w)] and 1: 9 [CMC@SNP: CNF (w/w)]. The result indicated that a sample at ratio 1:9 decreased the hydroxyl functional group, decreased in (C=O) O group, and increased C-H stretching, indicating a change in the water content and the sample at ratio 1:1 increased in the hydroxyl group and decreased the C=O group and C-H stretching.

Table (4) the result of FTIR before and after aging

Result	9:1		1:1		1:9		*Functional G*	Notes
	After	*Before*	*After*	*Before*	*After*	*Before*		
Best sample 1: 9	3382	3381	3277.70	3359	3319	3299	OH	The single bond 4000^{-1}-2500^{-1}
	2924.97	2923	2922.39	2927	2921	2919	C-H Stretching	
	2851.98	2852	2852.71	2854	2849	2851	CH stretching	
	1738.01	1738	1732.86	1794	1793.9	1795	Unconjugated C=O	
	1639.68	1638	1634.07	1626	1650	1642	O-H bending from absorbed water	Double bond 1500 cm^{-1} - 2000 cm^{-1}
	1587.39	1586	1540.11	-	1593	1592	Unconjugated C=O	
	1412	1415	1449	1407	1458	1422	CH_2 bending of pyranose ring	
	-	-	1383.11	-	1376	1375	C-H bending	-
	-	-	1177.91	1160	1173	1174	C-O-C	-
	872.31	871	870.94	871	899	897	β-glycosidic linkage between glucose units in cellulose	-

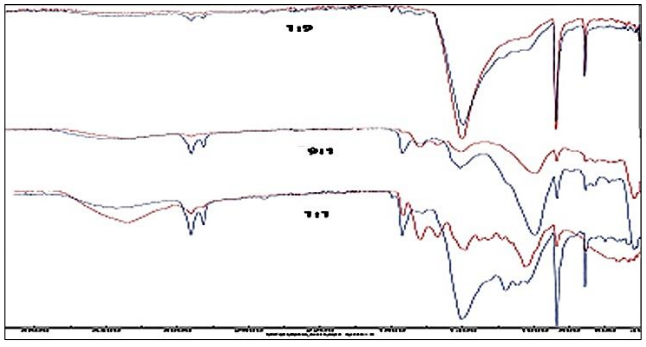

Figure (4) FTIR spectrum of samples treated after aging and untreated before aging by a different ratio

4. Case Study

The study was conducted on an archaeological painting that was strengthened by a nanocomposite CMC@SNP: CNF applied in a ratio of 9:1 for high penetration and homogenization of nanomaterials on the surface of the painting.

4.1. *Description of the painting*

A painting was applied to a canvas of the late twentieth century (25 cm×50 cm) in a frame represents. The oil painting was displayed on a wall next to the window. A painting was the still life of a dead duck, placed in front of a cauliflower, an apple, and a ceramic bowl on a table unsigned, but dated 1983 written on the front surface of the plate on the lower right side. The painting showed many signs of damage, such as fragility and weakness of the fibers, lacerations, cuts, cracks, and falling of the color crust, fig. (5).

Figure (5) the historical painting, and the area showing the painting date

4.2. *Documentation by photographs*

Photos showed dirt and dust on the front and back surface, a change in the colors and opacity of most parts of the panel, and the presence of cuts at the edges of the panel from the edges, cracks, and falling of the color crust at the edges of the panel from the bottom to the middle, fig. (6-a & b). There was also observed fading in some places, especially the red, beige, and green colors, and the weakness of the textile carrier was observed, fig. (6-c & d).

Figure (6) **a.** the back surface of the painting, damage and its impact on moisture, **b.** the falling of the paint crust and the weakness of the fabric, **c.** damage of the paint layer, as the darkening, falling paint layer, **d.** weak canvas, and twisting of threads of the canvas

4.3. *Microscopic examination*

The examination of the fibers with an optical microscope showed transverse marks and bulges along the fibers in the

longitudinal sector, and the general appearance (size, shape, and tapered- end) corresponds to linen, fig. (7-a). The fibers' loss of elasticity and fragility in several places, fig. (7-b), revealed the weakness of the canvas, cuts, and protrusion of the coating outside the cut, as demonstrated by examination of a cross-section of the layers by polarizing, fig. (7-c).

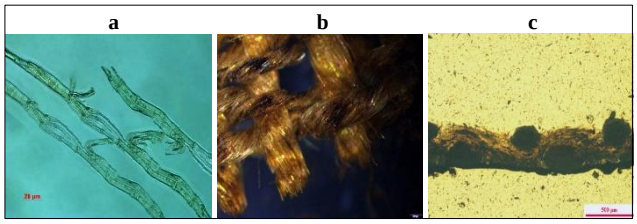

Figure (7) light microscopy photos show; **a.** weak linen fibers, **b.** brittle fiber, **c.** cross-section of layer canvas weak fibers

Stereo microscope examination of paint, fig. (8), of a sample of the blue color showed a change to green in some areas, cracks, flaking of the color, and darkening, fig. (8-a). A sample of the orange color showed cracks, dirt, and irregularity of the surface as fig. (8-b), while the brown color sample illustrated the cracked color layer, discoloration, hardening of the color crust, and weakening of the canvas, fig. (8-c).

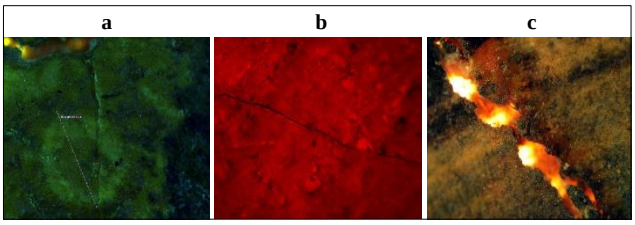

Figure (8) stereomicroscope examination; **a.** blue color sample, **b.** orange color sample, **c.** brown color sample

Polarizing microscope examination of a cross-section of the blue and brown colors, fig. (9), showed the weakness and decomposition of the blue color, discoloration, and weakness of the canvas as fig. (9-a). The structure of the layers appeared to consist of a weak canvas layer, a separate ground layer, a decomposition and cracked paint layer, and a varnish layer of the brown sample, fig. (9-b).

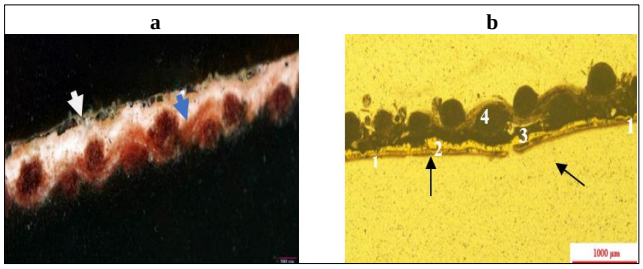

Figure (9) PM examination of a cross-section; **a.** a blue color sample show the hardness and the weak canvas, **b.** a brown color sample consisting of (1) varnish layer (2) paint layer (3) ground layer (4) canvas layer

SEM examination showed that the fibers of the canvas were weak and eroded, the irregularity of the canvas surface, and the cutting of the fibers, fig. (10-a & b). SEM examination showed the weakness and decomposition in the blue color sample, fig. (10-c) and the paint solid and cracked and lost paint in the orange color sample, fig. (10-d). It illustrated the fragility and weakness of the color layer of the brown color sample, fig. (10-e).

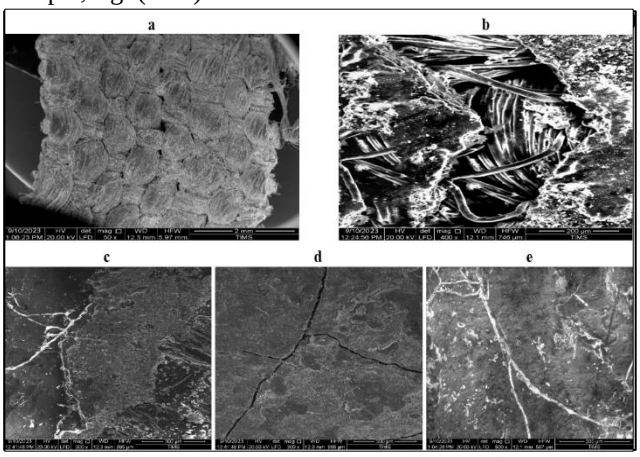

Figure (10) SEM photomicrographs; **a.** brittle and weak fibers, **b.** cutting of fibers and irregularity of the surface, **c.** the blue color sample by 300 X, **d.** the orange color sample by 300 X, **e.** the brown color sample by 500X

4.4. Paint layer analyses by EDX, Raman, and FTIR

EDX analysis of the blue color, fig. (11-a), showed that the sample consisted of oxygen (6.33%), carbon (15.3%), sulfur (1.15%), copper (75.19%), and chlorine (2.35%), indicating the color of azurite and malachite. *Raman* analysis, fig. (11-b) showed that the blue color was from azurite in the range of 155 cm^{-1}-190 cm^{-1}—272 cm^{-1}-363 cm^{-1}- 461 cm^{-1}-472 cm^{-1}- 1084 cm^{-1}- 1428 cm^{-1}- 762 cm^{-1}- 824 cm^{-1}- 855 cm^{-1} and malachite at the range of 155 cm^{-1}- 190 cm^{-1}- 352 cm^{-1}- 472 cm^{-1}-1084 cm^{-1}-1017 cm^{-1}-1173 cm^{-1}. The Raman analysis confirmed the EDX analysis that the blue sample was azurite. The Raman analysis confirmed the EDX analysis that the blue sample contained azurite and malachite. It confirmed the color change from azurite blue to malachite green [43].

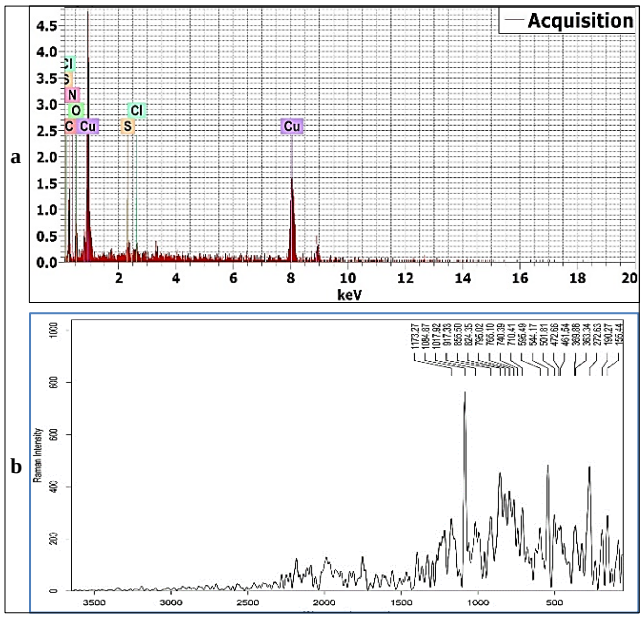

Figure (11) **a.** EDX pattern, **b.** Raman spectra of blue sample

The EDX analysis of the orange sample, fig. (12-a) showed that it consisted of oxygen (21.19%), carbon (30.46%), and barium (20.56%) in large proportions, as well as sulfur (9.42%), aluminum (0.62%), silica (2.48%), calcium (.051%), iron (2.52%), zinc (2.28%), chlorine (0.58%), mercury (2.77%), potassium (0.10%), and lead (7.06%). The analysis showed that the orange color was composed of vermilion red, red lead, and gothite yellow. The presence of calcium was because the ground is composed of calcium carbonate and due to the presence of potassium and silica due to gothite [44] because it is an earth oxide and has a percentage of alkaline substances from clay [45]. The Raman analysis, fig. (12-b) showed that the orange color was a mixture of vermilion red and lead red with gothite yellow. The Raman spectrum showed verm-ilion red at three main bands at 252 cm^{-1}, 270 cm^{-1}, and 337 cm^{-1} [46]. Furthermore, the Raman spectrum of ochre (III) showed 1135 cm^{-1} [48], 375 cm^{-1},1017 cm^{-1}, and 491 [47], 410sh, 652 cm^{-1}, 574 cm^{-1}, 676 cm^{-1}, 234 cm^{-1}, 1035 cm^{-1}, red hematite 270 cm^{-1}-,234 cm^{-1},667 cm^{-1}, 625 cm^{-1},603 cm^{-1} [49], 410 cm^{-1},460 cm^{-1}, and red lead at 1085 cm^{-1}, 574 cm^{-1}, 491, 460, 375, 316, 234, 190.

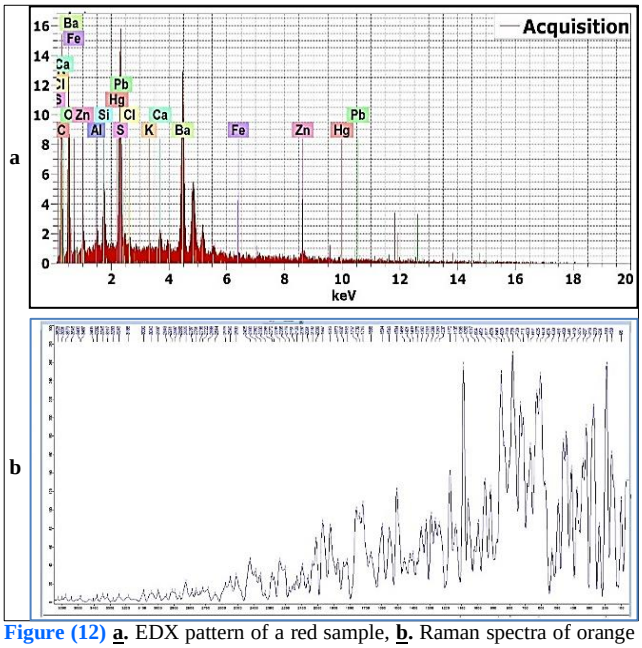

Figure (12) **a.** EDX pattern of a red sample, **b.** Raman spectra of orange sample

The analysis by the EDX unit of the brown color sample, fig. (13-a), showed that the sample consisted of carbon (75.43%) and oxygen (21.28%) as basic compounds, and sodium (0. 14%), magnesium (0.03%), aluminum (0.79%), silica (0.29 %), potassium (0.06%), calcium (8.3%), manganese (8.3%), iron (7.19%), copper (0.01%), cadmium (0.08%), gold (0. 56%), and lead (0.51%), illustrating the presence of iron oxide, manganese dioxide, silica and aluminum in the burnt umber and small proportions of Cu, Si, K, Cd, Pb, and Au. Calcium is considered impurities, and the presence of calcium and silica in the ground layer is explained by the sample of calcium carbonate. Additionally, the presence of lead with cadmium on the red of several types showed the mixture of red color with brown. The Raman analysis of the brown sample, fig. (13-b), showed the presence of burnt amber in the range of 1481-1617. The Raman analysis, fig. (13-c) confirmed the use of linseed oil as a binder because of the presence of the bands at the range of 3092, 1746, 1660, 1441, 1331, 1242, 985, 886, 446145, and 200. It confirmed the presence of the carbonate group at 156, 277, 716, and 1084, which led to the presence of calcium carbonate [50], and the presence of animal glue for the presence of the bands of the CH stretching group in the range of 2845-2932 and the bands of amid I at the range of 1644 and the amid II at the range of 1110. The analysis showed the presence of mastic varnish for the presence of the group V(C=O) at the ranges of 1687 and 1718, the group $\delta(CH_2)$, $\delta(CH_3)$ at the ranges of 1585, 1378, and 1317, the group δ(CH=CH) at the ranges of 1292, 1242, 1114, and 1136, the set v(c–c) ring at 1014, 1085, and 1084, the set δ(C–C) aromatic at 951, the set V(C–C–Oh) at 844, and the set v(c–c) ring at 749.

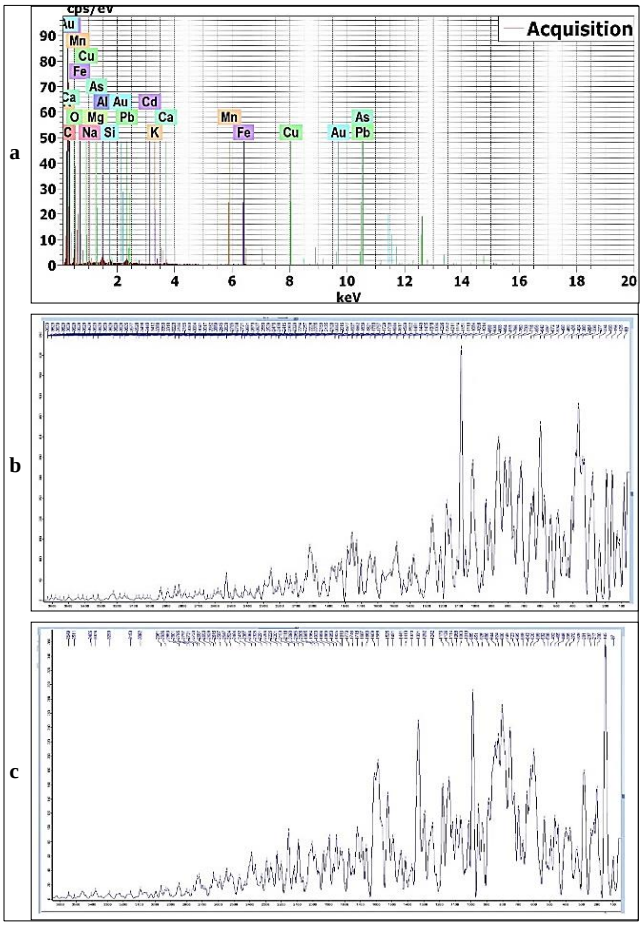

Figure (13) **a.** EDX pattern of the burnt umber, **b.** Raman spectra of brown sample, **c.** Raman spectra of medium & varnish

FTIR analysis confirmed the type of ground and adhesive as fig. (14) for the presence of the amide group (CN stretching & NH bending) at a wavenumber of 1586 cm^{-1} and the presence of the group (amid I, C-O stretch) at a wavenumber of 1630 cm-1, indicating that the adhesive was rabbit skin glue. Furthermore, the appearance of spectra of glue mixed

with calcium carbonate $CaCO_3$ at a wavenumber of 871 cm^{-1} for adsorption to carbonates and the presence of the carbonate group at a wavenumber of 1415 cm-1 demonstrated that the type of ground was a calcium carbonate mixed with glue. The analysis confirmed that the medium used was linseed oil due to the presence of a stretching band O-H group at a wave-number of 3381 cm^{-1}, νASCH2 absorption group stretching at a wavenumber of 2921 cm^{-1}, C=O (ester) stretching group at a wavenumber of 1738 cm^{-1}, and the CH_3 asymmetric bending absorption group at a wavenumber of 1415 cm^{-1}, which indicated the use of linseed oil [51]. The analysis proved that the varnish used was mastic for the presence of groups V (=C-H) at wavenumbers 3381 CM- 2921 and 2852, the group C=O stretching band at a wavenumber of 1738, the group C-C stretching band at a wavenumber of 1630, the group C-H bending bands at a wavenumber of 1415, and the group V (C=C) at a wavenumber of 997 [52].

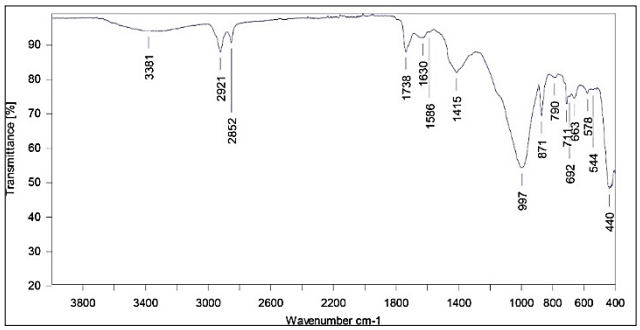

Figure (14) FTIR spectra of the medium and varnish

5. Discussion

Restoring oil paintings is a problem due to the nature of the chemical composition of the paintings. Restorers need to choose the restoration materials with high precision so as not to harm them. Nanomaterials are effective in restoring oil paintings even at low concentrations. Because of their small size, they penetrate the material to be treated well. The use of nanomaterials in consolidation and deacidification has increased [53]. The use of a nanocomposite consisting of a nanomaterial loaded on a polymer as [Sil /PEI/CMC: CNF/w:w] is one of the successful methods in the restoration of paintings based on the use of nanoparticles for mechanical reinforcement of the fibers as a material loaded on a polymer added with other compatible nanomaterials, which leads to the penetration of the treated material and a homogeneous surface, so the treated silica nanoparticles combining polyelectrolyte-treated silica nanoparticles (SNP) were used [54] with polyelectrolyte, PEI/CMC, and CNF for painting reinforcement. Nano-cellose was used in reinforcement mostly due to its unique mechanical properties and surface features, such as gas or lipid barrier, hydrophobic, antibacterial, and anti-UV. It has advantages in strong adhesiveness to stabilize the color peel, it does not cause color change, and it forms a transparent, lightweight film [55]. The success efficiency of nanocomposite [Sil/PEI/CMC:CNF/w:w] in different ratios (1:1, 9:1, and 1:9) applied to the experimental samples before and after thermal aging and light aging were demonstrated to reach the appropriate ratio for the reinforcement materials by SEM which indicated that there were no deposits on the surface of nanoparticles, suggesting that the nanoparticles penetrated the surface because this was helped by the presence [56] of a large amount of [CMC] which provides the production of films with higher elasticity, allowing for deeper migration and filling of cracks the fibers and the formation of homogeneous monolayer. This result confirmed the success of the 9:1 nanocomposite [57] compared to samples applied at a ratio of 1:1 and 1:9, which formed a surface layer. Silica appeared on the surface of the treated samples (indicated by white color), which indicated the lack of silica penetration and deposition on the surface, and the presence of a large percentage of CNF formed a cross-linked network on the surface [58], affecting the penetration of silica, which greatly increased the percentage of silica on the surface of the samples. pH measurement of the experimental samples with different mixing ratios showed that the ratio 1:9 changed pH, and the surface became alkaline because the decrease in silica concentration led to penetration into the surface. The CNF remained on the surface, forming an elastic film with increased CMC percentage, while the opposite occurred in other mixing ratios. Color measurements for the aged samples treated with Sil/PEI/CMC: CNF showed that color changes occurred with thermal and light aging for the sample's ratio of 9:1 change with a slight percentage. ΔE* was 0.8. For samples with a mixing ratio of 9:1/1:1, ΔE* was respectively 1.1 and 1.5. In addition, yellowing occurred in mixing ratios 1:9/1:1/ greater than the ratio 9:1. This was probably a result of degradation of the cationic polymer PEI, which tended to yellow upon thermal aging [59]. This enhanced the interactions between cellulose and the cationic polymer PEI, which increased yellowing. The lower color change observed for the experimental sample with a ratio of 9:1 might indicate that the CMC with a large ratio provided protection against the degradation of the cationic PEI polymer [60]. The tensile test showed the mechanical efficiency at a ratio of 1:9 because the CNF formed a thin layer on the surface, resulting in increased ductility. The SNP penetrated deeper and was strengthened throughout the layer, resulting in higher stiffness. The surface treated with Sil/PEI/CMC [61] was mechanically affected by aging due to the network of hydrogen bonds formed on the surface which would lead to mechanical improvement, as the previous hydrogen bond strengthened the network of cellulose nanoparticles and their interaction with textiles and the anionic polymer (carboxymethyl) cellulose (CMC), unlike other mixing ratios 1:9 /1:1 [62]. The infrared analysis indicated the functional groups that indicated whether changes occurred in the experimental study samples treated with nanomaterials before and after the photo and thermal aging process. It confirmed that in the sample treated at a ratio of 9:1, there was no change in the functional group because both the hydroxyl group and C-H stretching increased slightly compared to others, suggesting that the water content of the cellulose of the sample was not affected. Also, there was no change in the C=O mixture, which indicated no effect on the hemicellulose group [63]. In contrast, there was a change in the

functional group in the samples mixed at ratios of 1:1 and 1:9, indicating a change in the water content of the sample. The results of examinations and analyses of the historical painting showed that it had much damage, as proved by optical microscopy (OM), stereo, SEM, and polarized examination. The fibers of the linen fabric were weak and frayed, and there were cuts at the edges of the painting, cracks, and loss of color peel. It was noted that the fabric was fragile and uneven. The layered structure showed the extreme weakness of the panel layers and the weakness of the fibers, which confirmed the necessity of strengthening and lining the painting.

6. Restoration Processes of the Case study

6.1. *Consolidation using nanocomposite and lining*

The front and back surface of the painting was cleaned with a soft brush, and the surface was protected by Japanese paper using a brush after the weak color crust was fixed from the bottom by injection, as shown in fig. (15-a & b). The installation was conducted with nanocomposite 9%CMC@SNP : 1%CNF by 2.5% dissolved in 100 ml of ethanol, then ironed and cauterized with a thermal iron at 45 °C, fig. (15-c). After protection and fixing the weak color crust, the canvas was uniformly re-straightened from the back surface to ensure that the torn parts did not separate [64], fig. (15-d) and was done on the edges of the painting because of their weakness.

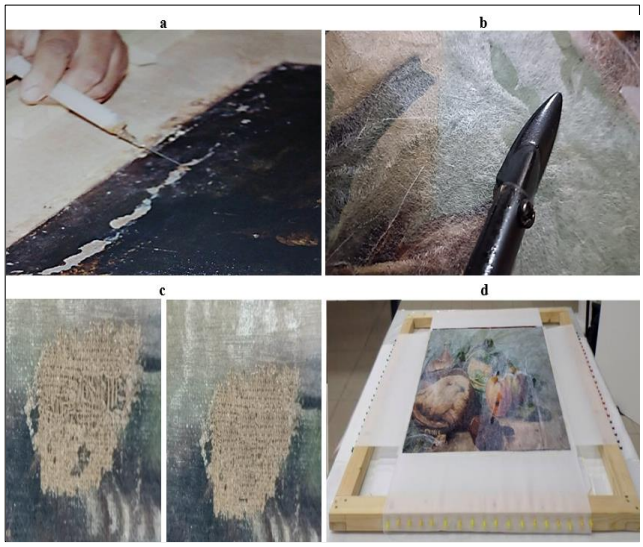

Figure (15) the fixation of the paint that was about to **a.** fall, **b.** with heat, **c.** restoring the position of the fabric fibers and flattening the area, **d.** protecting the surface paint and making the sides of the painting

The cut parts were fixed using nanomaterial compound adhesive and Nantacid paper, characterized by flexibility. It is a paper made of non-woven, high-density polyethylene fibers. It does not expand or tear, and it maintains its physical properties during humidity vibration [65]. Ironing and light pressure were applied to flatten and enhance adhesion, fig. (16-a). Then, weights were placed on it and left for 24 hours. The back surface of the original canvas of the painting was cleaned with a nano compound to remove the acidity and left for 48 hours. After that, the lining process was carried out using the cold lining method using 2% plexitol dissolved in xylene and two wooden frames with Belgian linen fabric stretched over them. The first frame was made of new wood with a size larger than the original painting, and the other frame was larger than the first by 10 cm on each side. The size of the painting was determined by number (2), which was stretched with linen and painted with plexitol to the specified size, which was applied with a brush. The original painting was painted from the back. The area painted with xylene was sprayed on the new canvas and the original painting surface. Then, the painting was applied to No. "1" inside No. 2", fig. (16-b). Next, it was placed on a surface, and suitable weights were placed on it until the next day. Then, the painting was tightened onto the original stretch wood after cleaning and sterilizing. The Japanese paper was removed from the drywall carefully by hand. When adhered parts were found, they were wet with distilled water and then raised so that they were parallel to the surface.

Figure (16) **a.** the application of the painting inside the stretch wood; "No 2", **b.** patching the cut parts using Nantacid paper and ironing.

6.2. *Cleaning process*

Mechanical cleaning was carried out using soft brushes and then cleaning with an enzyme with natural saliva, which dissolved part of the surface dirt and removed paint particles by mechanical action without damaging the paint layer [66]. Then, solvent cleaning used a mixture of isopropyl solvent with white Sprite solvent in a ratio of 1:1 that worked effectively in cleaning the light areas of the painting, fig. (17-a). The old varnishes were cleaned with a solvent mixture consisting of white Sprite: isopropyl in a ratio of (1: 3) or (5: 5), fig. (17-b).

Figure (17) **a.** the cleaning of the right side of the painting, **b.** the use of cleaning with a mixture of solvents

6.3. *Filling & retouching*

The missing parts of the ground layer were filled using a white paste consisting of calcium carbonate + one part glue + 9 parts

water. Then, the putty area was smoothed using a piece of soft sandpaper. The retouch was done using colors type Maymeri.

6.4. *Restoration of the frame*

The frame was cleaned mechanically, using a soft brush to remove simple dust, then the saliva enzyme, simple to remove the non-simple dust. Then cleaning by chemical methods using vegetable turpentine solvent, the cleaning rates were weak, then cleaning with ethyl alcohol, the cleaning rates were weak, then cleaning with a mixture consisting of ethyl alcohol + vegetable turpentine in a ratio of 2:1. It was found that cleaning with this mixture gives a better result than all the previous solvents.

6.5. *Applying the varnish*

After the retouch dried, the varnish types Gamvar Satin/ Matte Picture, Manufacturer/Supplier Gamblin Artists Color, was applied to the surface by spraying with a gun. which is transparent and does not change color, and the painting was put in the frame, fig. (18).

Figure (18) the painting **a.** before and **b.** after restoration.

7. Conclusion

Consolidation by green nanocomposite is preferred in restoring oil paint applied on canvas. The green nanocomposite based on combinations of SNP and CNF treated with CMC is suitable for treating the loss of mechanical integrity of deteriorated canvas. The reinforcement properties of the formulations can be adjusted by changing the ratio between silica and CNF particles. Due to the size difference between the components, the green nanocomposite [Sil/PEI/CMC: CNF/ w:w] at ratios of 9:1, 1:9, and 1:1 provided suitable treatment. A comparison revealed that the green nanocomposite [Sil/PEI/CMC: CNF/ w:w] mixed at a ratio of 9:1 provided the best results in strengthening and removing acidity. CNF formed a thin layer on the surface of the fabric, while silica particles penetrated the interior of the fabric. The high CNF content in the formulation resulted in ductile behavior, while the high silica content resulted in a stiffer fabric and provided the potential to reinforce the deteriorating panel compared to other processors at a ratio of 1:1/1:9.

Acknowledgment

We extend our sincere thanks and appreciation to Dr. Rasha Kamel at the Spectral Analysis Unit, the Saad Zaghloul Center at the Antiquities Authority, and Dr. Abu Al-Hamad, Prof. at the Chemistry dept., Faculty of Science, Aswan Univ.

References

[1] Hendrickx, R., Desmarais, G., Weder, M., et al., (2016). Moisture uptake and permeability of canvas paintings and their components. *J. of Cultural Heritage*.19: 445-453.

[2] Stoner, J. & Rushfield, R. (2012). *The conservation of easel paintings*, Routledge, NY.

[3] Ploeger, R., De La Rie, E., McGlinchey, C., et al., (2014). The long-term stability of a popular heat-seal adhesive for the conservation of painted cultural objects. *Polymer Degradation & Stability*.107: 307-313.

[4] Chelazzi, D., Chevalier, A., Pizzorusso, G., et al., (2014). Characterization and degradation of poly (vinyl acetate) based adhesives for canvas paintings. *Polymer Degradation & Stability*. 107: 314-320.

[5] Ackroyd, P. (2002). The structural conservation of canvas paintings: Changes in attitude and practice since the early 1970s. *Studies in Conservation*. 47: 3-14.

[6] Ackroyd, P., Phenix, A. & Villers, C., (2002). Not lining in the twenty-first century: Attitudes to the structural conservation of canvas paintings, *The Conservator*. (1): 14-23.

[7] Mahfuz, H., Clements, F., Rangari, V., et al. (2009). Enhanced stab resistance of armor composites with functionalized silica nanoparticles. J. *of Applied Physics*. 105 (6), doi: 10.1063/1.3086431.

[8] Bonini, M., Lenz, S., Giorgi, R., et al. (2007). Nanomagnetic sponges for the cleaning of works of art. *Langmuir*. 23 (17): 8681-8685.

[9] Giorgi, R., Chelazzi, D. & Baglioni, P. (2005). Nanoparticles of calcium hydroxide for wood conservation: The deacidification of the vasa warship. *Langmuir*. 21 (23): 10743-10748.

[10] Baglioni, P., Chelazzi, D. & Giorgi, R. (2015). *Nanotechnologies in the conservation of cultural heritage: A compendium of materials and techniques*, Springer, The Netherlands.

[11] Giorgi, R., Bozzi, C., Dei, L., et al., (2005). Nanoparticles of Mg (OH) 2: Synthesis and application to paper conservation. *Langmuir*. 21 (18): 8495-8501.

[12] Mahltig, B., Swaboda, C., Roessler, A., et al., (2008). Functionalising wood by nanosol application. J. *of Mat erials Chemistry*.18 (27) : 3180-3192.

[13] Schollmeyer, E., Zorjanović, J., Textor, T., et al., (2007). Nanotechnology for functionalization of textile materials. *Tekstil-Zagreb*. 56 (2): 75-86.

[14] Afsharpour, M. & Hadadi, M., (2014). Titanium dioxide thin film: Environmental control for preservation of paper-artworks. *J. of Cultural Heritage*. 15 (5): 569-574.

[15] Periyasamy, A., Venkataraman, M., Kremenakova, D., et al. (2020). Progress in sol-gel technology for the coatings of fabrics. *Materials*. 13 (8), doi: 10.3390/ma 13081838

[16] Howe, A., Wesley, R., Bertrand, M., et al. (2006). Controlled association in suspensions of charged nanoparticles with a Weak Polyelectrolyte. *Langmuir*. 22 (10): 4518-4525.

[17] Bauer, D., Killmann, E. & Jaeger, W. (1998). flocculation and stabilization of colloidal silica by the adsorption of poly-diallyl-dimethyl-ammoniumchloride (pdadmac) and of copolymers of dadmac with n-methyl-n-vinyl-acetamide (NMVA). *Colloid & Polymer Science*. 276: 698-708.

[18] Gregory, J. & Barany, S. (2011). Adsorption and flocculation by polymers and polymer mixtures. *Advances in Colloid & Interface Science*.169 (1), doi: 10.1016/j. cis.2011.06.004.

[19] Moon, R., Martini, A., Nairn, J., et al. (2011). Cellulose nanomaterials review: Structure, properties and nanocomposites. *Chemical Society Reviews*. 40 (7): 3941-3994.

[20] Nechyporchuk, O., Belgacem, M. & Pignon, F. (2016). Current progress in rheology of cellulose nanofibril suspensions, *Biomacromolecules*. 17 (7): 2311-2320.

[21] Stevens, M. (1990). *Polymer Chemistry* 2, Oxford Univ. Press, NY.

[22] Dreyfuss-Deseigne, R. (2017). Nanocellulose films in art conservation: A new and promising mending material for translucent paper objects. *J. of Paper Conservation*. 18 (1): 18-29.

[23] Santos, S., Carbajo, J., Gómez, N., et al. (2016). Use of bacterial cellulose in degraded paper restoration. Part I: application on model papers. *J. of Materials Science*. 51 (3): 1541-1552.

[24] Anghelone, M., Jembrih-Simbürger, D., Pintus, V., et al. (2017). Photostability and influence of phthalocyanine pigments on the photodegradation of acrylic paints under accelerated solar radiation. *Polymer Degradation & Stability*. 146: 13-23.

[25] Rahimi, M. & Behrooz, R. (2011). Effect of cellulose characteristic and hydrolyze conditions on morphology and size of nanocrystal cellulose extracted from wheat straw. *Int. J. of Polymeric Materials*. 60 (8): 529-541.

[26] Kim, Y., Lee, S., Lee, E., et al. (2014). Toxicity of colloidal silica nanoparticles administered orally for 90 days in rats. *Int. J. of Nanomedicine*. 9: 67-78.

[27] Tan, V., Tay, T., Teo, W. (2005). Strengthening fabric armour with silica colloidal suspensions. *Int. J. of Solids & Structures*. 42 (5-6): 1561-1576.

[28] Mahltig, B., Haufe, H. & Böttcher, H. (2005). Functionalization of textiles by inorganic sol-gel coatings. J. of Materials Chemistry. 15 (41): 4385-4398.

[29] Dreyfuss-Deseigne, R. (2017). Nanocellulose films in art conservation: A new and promising mending material for translucent paper objects. *J. of Paper Conservation*. 18 (1): 18-29.

[30] Völkel, L., Ahn, K., Hähner, U., et al. (2017). Nano meets the sheet: Adhesive-free application of nanocellulosic suspensions in paper conservation. *Heritage Science*. 5, doi: 10.1186/s40494-017-0134-5.

[31] Nechyporchuk, O., Kolman, K., Bridarolli, A., et al. (2018). On the potential of using nanocellulose for consolidation of painting canvases. *Carbohydrate Polymers*. 194: 161-169.

[32] Cherian, R., Tharayil, A., Varghese, R., et al. (2022). A review of the emerging applications of nano-cellulose as advanced coatings. *Carbohydrate Polymers*. 282: 119-123.

[33] Rentzhog, M. & Fogden, A. (2005). Influence of formulation and properties of water-based flexographic inks on printing performance for pe-coated board, *Nordic Pulp & Paper Research J*. 20 (4): 410-417.

[34] Ackroyd, P., Phenix, A. & Villers, C. (2002). Not lining in the twenty-first century: Attitudes to the structural conservation of canvas paintings. *The Conservator*. 26 (1 14-23.

[35] Carretti, E., Dei, L., Weiss, R., et al. (2008). A new class of gels for the conservation of painted surfaces. *J. of Cultural Heritage*. 9 (4): 386-393.

[36] Liu, W., Liu, K., Du, H., et al. (2022). Cellulose nanopaper: Fabrication, functionalization, and applications. *Nano-Micro Letters*.14 (104), doi: 10.1007/s40820-022-00849-x.

[37] Zhong, J., Zhu, H., Zhong, Q., et al. (2015). Self-powered human-interactive transparent nanopaper systems. *ACS Nano*. 9 (7): 7399-7406.

[38] Young, C. & Hibberd, R. (1999). Biaxial tensile testing of paintings on canvas. *Studies in Conservation*. 44 (2): 129-141.

[39] Havlínová, B., Katuščák, S., Petrovičová, M., et al. (2009). A Study of mechanical properties of papers exposed to various methods of accelerated ageing. Part I. the effect of heat and humidity on original wood-pulp papers. *J. of Cultural Heritage*. 10 (2): 222-231.

[40] Baglioni, P., Giorgi, R. & Chelazzi, D. (2012). Nanomaterials for the conservation and preservation of movable and immovable artworks. *Int. J. of Heritage in the Digital Era*. 1 (1): 313-318.

[41] Böhme, N., Anders, M., Reichelt, T., et al. (2020). New treatments for canvas consolidation and conservation, *Heritage Science*. 8 (1), doi: 10.1186/s40494-020-0362-y.

[42] Baglioni, P., Chelazzi, D., Giorgi, R., et al. (2015). Deacidification of paper, canvas and wood, Ch. 5. In: Baglioni, P., Chelazzi, D., Giorgi, R., et al. (eds.) *Nanotechnologies in the Conservation of Cultural Heritage: A Compendium of Materials and Techniques*, Springer, The Netherlands, pp. 117-144.

[43] Naumova, M. & Pisareva, S. (1994). A note on the use of blue and green copper compounds in paintings. *Studies in Conservation*.39 (4): 277-283.

[44] Pervukhina, N., Romanenko, G., Borisov, S., et al. (1999). Crystal chemistry of mercury (I) and mercury (I, II) minerals. J. *of Structural Chemistry*. 40: 461-476.

[45] Hall, K., Meiklejohn, I. & Arocena, J. (2007). The thermal responses of rock art pigments: Implications for rock art weathering in southern Africa. *Geomorphology*. 91 (1-2): 132-145.

[46] Bouchard, M. & Smith, D. (2003). Catalogue of 45 reference raman spectra of minerals concerning research in art history or archaeology, especially on corroded metals and coloured glass. *Spectrochimica Acta Part A: Molecular and Biomolecular Spectroscopy*. 59 (10): 2247-2266

[47] Mastrotheodoros, G. & Beltsios, K. (2022). Pigments—iron-based red, yellow, and brown ochres. *Archaeological & Anthropological Sciences*. 14, doi: 10.1007/s12520-021-01482-2.

[48] Thibeau, R., Brown, C. & Heidersbach, R. (1978). Raman spectra of possible corrosion products of iron. *Applied Spectroscopy*. 32 (6): 532-535.

[49] Nyström, I. (2015). Spectroscopic analysis of artists' pigments and materials used in southern swedish painted wall hangings from the eighteenth and nineteenth centuries. *Studies in Conservation*. 60 (6): 353-367.

[50] Van der Weerd, J., Smith, G., Firth, S., et al. (2004). Identification of black pigments on prehistoric southwest american potsherds by infrared and raman microscopy. *J. of Archaeological Science*. 31 (10): 1429-1437.

[51] Salvadó, N., Pradell, T., Pantos, E., et al. (2002). Identification of copper-based green pigments in jaume huguet's gothic altarpieces by fourier transform infrared microspectroscopy and synchrotron radiation x-ray diffraction. *J. of Synchrotron Radiation*. 9 (4): 215-222.

[52] Azémard, C., Vieillescazes, C. & Ménager, M. (2014). Effect of photodegradation on the identification of natural varnishes by FT-IR *Spectroscopy, Microchemical J*. 112: 137-149.

[53] O Völkel, L., Ahn, K., Hähner, U., et al. (2017). Nano meets the sheet: Adhesive-free application of nanocellulosic suspensions in paper conservation. *Heritage Science*. 5, doi: 10.1186/s40494-017-0134-5.

[54] Le, V., Thuc, C. & Thuc, H. (2013). Synthesis of silica nanoparticles from vietnamese rice husk by sol-gel method. *Nanoscale Research Letters*. 8, doi: 10.1186/1556-276X-8-58.

[55] Rahimi, M. & Behrooz, R. (2011). Effect of cellulose characteristic and hydrolyze conditions on morphology and size of nanocrystal cellulose extracted from wheat straw. *Int. J. of Polymeric Materials and Polymeric Biomaterials*. 60 (8): 529-541.

[56] Operamolla, A., Mazzuca, C., Capodieci, L., et al., (2021). Toward a reversible consolidation of paper materials using cellulose nanocrystals. *ACS Applied* Materials *& Interfaces*. 13 (37): 44972-44982.

[57] Cherian, R., Tharayil, A., Varghese, R., et al., (2022). A review of the emerging applications of nano-cellulose as advanced coatings. *Carbohydrate Polymers*. 282: 119-123.

[58] Bridarolli, A., Nechyporchuk, O., Odlyha, M., et al. (2018). Nanocellulose-based materials for the reinforcement of modern canvas-supported paintings. *Studies in Conservation*. 63 (S1): S332-S334.

[59] Vinogradova, S. Korshak, V., Kul'chitskii, V., et al. (1968). Thermal stability of unsaturated polyesters and copolymers based on them. *Polymer Science USSR*. 10 (7): 1757-1764.

[60] Siqueira, E., Salon, M., Belgacem, M., et al. (2015). Carboxymethylcellulose (CMC) as a model compound of cellulose fibers and polyamideamine epichlorohydrin (pae)–cmc interactions as a model of pae–fibers interactions of pae-based wet strength papers. *J. of Applied Polymer Science*. 132 (26), doi: 10.1002/app.42144.

[61] Arici, A. (2007). Effect of hygrothermal aging on polyetherimide composites. *J. of Reinforced Plastics & Composites*. 26 (18): 1937-1942.

[62] Bridarolli, A., Odlyha, M., Burca, G., et al. (2021). Controlled environment neutron radiography of moisture sorption/desorption in nanocellulose-treated cotton painting canvases. *ACS Applied Polymer Materials* .3 (2): 777-788.

[63] Geminiani, L., Campione, F., Corti, C., et al. (2022). Differentiating between natural and modified cellulosic fibres using atr-ftir spectroscopy. *Heritage*. 5 (4): 4114-4139.

[64] Seymour, K. & Och, J. (2005). A *cold lining technique for large-scale paintings: Big pictures, problems and solutions for treating outsize paintings*, Archetype Pub., London.

[65] Phenix, A., (1985). Lining without heat or moisture. *The Conservator*. 9 (1): 45-46.